Published by :
http://www.ijert.org

International Journal of Engineering Research & Technology (IJERT)
ISSN: 2278-0181
Vol. 14 Issue 09, September - 2025

Performance Analysis of Solar Tracking Systems in Nigeria for Efficient Power Supply: Modelling and Simulation with PID and Fuzzy Logic Controller

Barisuka Uebari, D.O. Dike, L.O. Uzoechi, S. O. Okozi
Department of Electrical and Electronic Engineering
School of Electrical Systems Engineering and Technology
Federal University of Technology, Owerri
Imo State, Nigeria

Abstract: **Nigeria's frequent power outages highlight the need to find efficient ways to use renewable energy. In order to evaluate the performance of solar tracking systems in comparison to fixed-axis photovoltaic (PV) arrays under Nigerian irradiance conditions, this study models and simulates them using Proportional–Integral–Derivative (PID) and Fuzzy Logic Controllers (FLC) in MATLAB/Simulink. The findings indicate that PID-based two-axis tracking could produce 15.05A and 73.40V, whereas fixed-axis PV systems could only produce 7.39A and 46.55V at most. The FLC-using tracker consistently outperformed the other two. It operated better in the morning and at night when the sun was not as bright, and it received 22.32A and 109.93V at noon. The findings imply that because fuzzy logic control can better adjust to variations in irradiance, it is the better option for increasing solar energy capture. Using two-axis trackers based on FLC is the simplest way to maximise the performance of solar panels and boost the amount of renewable energy in Nigeria.**

Keywords: **Solar tracking systems, Proportional–Integral–Derivative (PID) controllers, Fuzzy logic controllers, MATLAB/Simulink, Photovoltaic (PV) arrays, Irradiance variability, Nigeria**

I. INTRODUCTION

The necessity of a stable electricity supply in Nigeria is paramount, as it is essential for social and economic development. Nigeria's persistent electricity deficit, marked by recurrent outages, inadequate grid reliability, and significant reliance on fossil fuel generation, remains a barrier to economic growth and social development [1]. Nigeria is located in one of the world's most solar-rich regions, receiving significant direct and global irradiance throughout the year.

Conventional fixed photovoltaic (PV) arrays are simple and low-cost but lose substantial potential energy because panel orientation is optimal only for a small portion of the day. Solar tracking systems (single-axis and dual-axis) address this limitation by continuously reorienting PV modules toward the sun, often providing measurable energy gains over fixed systems; however, those gains are sensitive to tracking strategy, actuator energy consumption and local climatic variability [2], [3]. Simulations using MATLAB/Simulink, PVsyst and other platforms allow rigorous evaluation of these control strategies across a range of irradiance patterns and mechanical constraints without costly field prototypes [4].

Despite the global literature demonstrating the promise of intelligent tracking controllers, regional studies specific to Nigeria are comparatively few and often do not simultaneously account for (a) the energy cost of actuation, (b) local irradiance variability, and (c) trade-offs between simple tuned PID controllers and rule-based fuzzy logic controllers. This study, therefore, develops detailed mathematical models and MATLAB/Simulink simulations of solar tracking systems employing PID and Fuzzy Logic controllers. It evaluates their performance under representative Nigerian irradiance profiles.

II. LITERATURE REVIEW

[5] showed that fuzzy logic controllers are superior to traditional PID controllers in managing nonlinearities and uncertainties in sun trajectory prediction. [6] examined hybrid PID–fuzzy controllers and found that hybridization enhances transient responses and tracking efficiency relative to standalone PID controllers. The findings are consistent with [7] who emphasized that fuzzy systems, owing to their rule-based adaptability, reduce steady-state error more efficiently than linear controllers. [8] demonstrated that ANFIS controllers, when trained with irradiance data, adapt dynamically to environmental changes and consistently exceed the performance of classical fuzzy systems. [9] noted that computational complexity and hardware costs could impede the widespread adoption of ANFIS in resource-constrained areas. [10] created a dual-axis tracker utilizing Simulink, incorporating PID and fuzzy control. Their findings indicated that the fuzzy-controlled model achieved superior power output in conditions of variable irradiance. [11] conducted a simulation of a solar tracker in MATLAB utilizing actual meteorological datasets from sub-Saharan Africa, demonstrating that intelligent controllers enhance daily energy harvest by

International Journal of Engineering Research & Technology (IJERT)
ISSN: 2278-0181
Vol. 14 Issue 09, September - 2025

15–20% relative to fixed systems. [12] utilized particle swarm optimization (PSO) for tuning PID gains in MATLAB, demonstrating improved convergence speed and decreased overshoot relative to Ziegler–Nichols tuning. [13] demonstrated that fuzzy–GA hybrid tuning attained enhanced accuracy in the context of highly variable Nigerian irradiance profiles. [14] examined fault conditions, including actuator stalling and sensor drift, to evaluate the resilience of PID and fuzzy controllers. [15] developed a microcontroller-based fuzzy solar tracker in Pakistan, demonstrating a 28% increase in energy output relative to fixed photovoltaic panels. [16] conducted an evaluation of a PID-controlled dual-axis tracker in northern Nigeria, reporting a 22% increase in energy efficiency while also noting difficulties in calibration due to dust accumulation and elevated ambient temperatures. [11] highlighted the effective incorporation of low-cost sensors and actuators, illustrating that economical fuzzy-based trackers can function effectively in off-grid rural environments. [17] conducted a year-long field trial of hybrid PID–fuzzy trackers in India, demonstrating energy yield improvements of 20–25% compared to fixed arrays, even in the face of seasonal variability. [16] present one of the limited experimental studies grounded in local context, as the majority of existing literature depends on simulations or field trials conducted in other developing countries. Moreover, [13] indicate that optimization strategies specifically designed for Nigeria's distinct irradiance variations and recurrent grid instability remain insufficiently investigated. [9] noted that hardware constraints and significant computational requirements could hinder rural electrification initiatives in Nigeria.

III. MATHEMATICAL MODEL

A. Modelling of PV Array System and Solar Tracking Angles

Considering a PV solar cell shown in Figure 1, the equivalent circuit which mathematically describes the I-V characteristics of the PV circuit is represented in Equation 1.

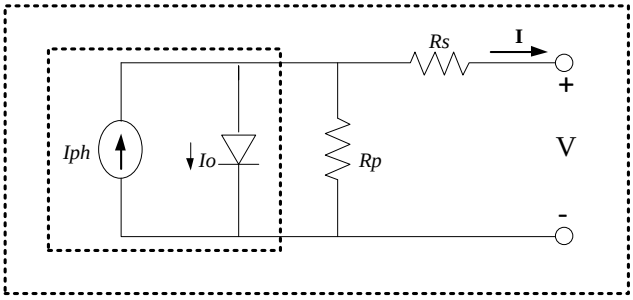

Figure 1: Single diode model circuit [18]

$$I = I_{ph} - I_o\left[exp\left(\frac{V+R_sI}{CV_ba}\right) - 1\right] - \frac{V+R_sI}{R_p} \quad (1)$$

Where R_s is the series resistance, R_p is the resistance in parallel a is the diode ideality constant, V_b is the thermal voltage of the solar cell, I_o is the diode saturation current, and R_{ph} is the photovoltaic (light-generated) current.

Diode ideality factor is the measure of how much a practical diode deviates from ideal diode equation. The average value assumed during the determination of unknown parameters in the photovoltaic system is usually 1.3. Also, the thermal voltage is a characteristic voltage that relates current flow in the p-n junction to the electrostatic potential across it, and is given

$$V_b = \frac{kT_n}{q} \quad (2)$$

Where k is Boltzmann constant ($1.3806503 \times 10^{-23}$ J/K), q is electron charge ($1.607 \times 10^{-19}\ C$), and T_n is nominal temperature (298.15K).

The light-generated current of the photovoltaic cell depends linearly on the solar irradiation and is also influenced by the temperature, and their relationship is given in Equation

$$I_{ph} = \left(I_{phn} + K_{cu}\Delta_T\right)\left(\frac{G}{G_n}\right) \quad (3)$$

I_{phn}, light generated current in solar cell circuit at nominal conditions (when temperature is 25°C and irradiance of 1000 W/m^2), K_{cu} is current temperature coefficient, $\Delta_T = T - T_n$, T is actual temperature and T_n is the nominal temperature, G is the actual sun irradiation and G_n is the nominal sun irradiation (usually 1000 W/m^2). The diode saturation current I_o and its dependence on the temperature may be expressed as

International Journal of Engineering Research & Technology (IJERT)
ISSN: 2278-0181
Vol. 14 Issue 09, September - 2025

$$I_o = I_{on}\left(\frac{T_n}{T}\right)^3 exp\left[\frac{qE_g}{ak}\left(\frac{1}{T}-\frac{1}{Tn}\right)\right] \quad (4)$$

Where, E_g is band gap energy of semiconductor $E_g = 1.12$ eV for the polycrystalline Si at 25°C.
Where I_{on} is given by the relationship in Equation 4

$$I_{on} = \frac{I_{sc}}{exp\left(\frac{V_{oc}}{CaV_b}\right)-1} \quad (5)$$

And I_{sc} is the short-circuit current, and V_{oc} open circuit voltage, respectively.
The elevation angle β is the angle between the sun rays and the horizontal surface (solar panel)

$$\sin\beta = \sin\delta\sin L + \cos\delta\cos L\cos\varepsilon \quad (6)$$

$$\theta_z = 90^0 - \beta \quad (7)$$

where L the latitude angle of the location is, δ is the declination angle, and ε is the hour angle.
The accuracy of the declination angles is important in navigation and astronomy. However, an approximation accurate to within 1 degree is adequate in many solar purposes. One such approximation for the declination angle is $\delta = \sin^{-1}\{0.39795\cos[0.98563(N-173)]\}\,(degrees)$ (8)
where N is day number and calendar dates are expressed as the $N = 1$, starting with January 1 $\varepsilon = 15(t_s - 12)$ (9)
where t_s is the solar time in hours. A solar time is a 24-hour clock with 12:00 as the exact time when the sun is at the highest point in the sky. the azimuth angle can be expressed as in equation 10 for True Local Time >12.00hr (Roth, Georgiev and Boudinov, 2009).

$$\emptyset = 180^o + \cos^{-1}\left(\frac{\sin\beta\sin L-\sin\delta}{\cos\beta\cos L}\right) \quad (10)$$

The azimuth angle for True Local Time <12.00hr is expressed as in Equation 11,

$$\emptyset = 180^o - \cos^{-1}\left(\frac{\sin\beta\sin L-\sin\delta}{\cos\beta\cos L}\right) \quad (11)$$

Where L is the latitude of the location, β is the elevation angle and δ is the declination angle.

$$H = \left|\frac{1}{15}\cos^{-1}\left[-\tan(L)\tan\left(23.44\sin\left(360\frac{(D+284)}{365}\right)\right)\right]\right| \quad (12)$$

Total irradiance on any inclined surface is the sum of direct irradiance, isotropic sky diffuse irradiance, and ground reflection as given in Equation 13

$$G = G_{bh}\frac{\cos\theta}{\cos\theta_z} + G_{dh}\frac{1+\cos\beta}{2} + G_h\rho\frac{1-\cos\beta}{2} \quad (13)$$

A DC motor was chosen as the actuator for the tracker. This motor moves the solar panel system along both the East/West and North/South axes. To create a model for the motor, its electrical and mechanical aspects are considered. Using Figure 2 and defining the angular twist of the shaft, the motor's differential equations can be found.

B. Modelling of Solar Tracker Drive Mechanism

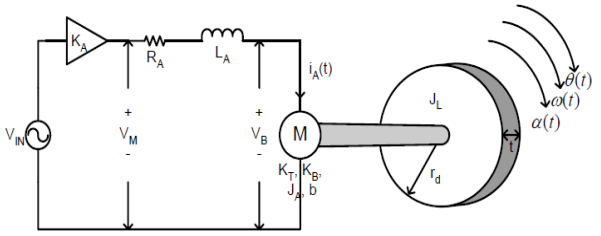

Figure 2: DC motor representation

Applying Kirchhoff's current and voltage laws, the electrical system equations are thus expressed as

International Journal of Engineering Research & Technology (IJERT)
ISSN: 2278-0181
Vol. 14 Issue 09, September - 2025

$$V_M(t) = K_A V_{IN}(t) \quad (14)$$

$$V_M(t) = i_A(t)R_A + L_A\frac{di_A(t)}{dt} + V_B(t) \quad (15)$$

Then,

$$V_B = K_B\omega_b(t) = K_B\frac{d\vartheta(t)}{dt} \quad (16)$$

In this context, let K_A denote the amplifier voltage gain, V_M the motor input voltage, $R_A$the motor armature coil resistance, L_A the motor armature coil inductance, i_A the motor armature coil current, V_B the motor back electromotive force (EMF), K_B the motor back EMF constant, ω_b the motor shaft angular velocity, and ϑ the motor shaft position.
The mechanical system includes the following differential equations

$$T(t) = K_T i_A(t) \quad (17)$$

$$T(t) = J_T \propto_a (t) + b\omega_b(t) = J_T\frac{d^2\vartheta(t)}{dt^2} + b\frac{d\vartheta}{dt} \quad (18)$$

where, K_T is motor torque constant, $\propto_a$ is the motor shaft angular acceleration, and J_T is the total inertia acting on the shaft, which includes the motor armature inertia, gear train inertia, and the solar panels' inertia.
Substituting Equations 14 and 15 in 16, we obtain

$$K_A V_{IN}(t) = i_A(t)R_A + L_A\frac{di_A(t)}{dt} + K_B\frac{d\vartheta(t)}{dt} \quad (19)$$

Also, substituting Equation 17 into 18, we have

$$K_T i_A(t) = J_T\frac{d^2\vartheta(t)}{dt^2} + b\frac{d\vartheta}{dt} \quad (20)$$

Applying Laplace transforms to Equations 19 and 20,

$$K_A V_{IN}(s) = I_A(s)R_A + L_A s I_A(s) + K_B s\vartheta(s) \quad (21)$$

$$K_T I_A(s) = J_T s^2\vartheta(s) + bs\vartheta(s) \quad (22)$$

Making I_A subject of the formula in Equation 22 and substituting the same in Equation 22, the final transfer function for the solar tracker drive mechanism is expressed as

$$\frac{\vartheta(s)}{V_{IN}(s)} = \frac{K_T K_A}{J_T L_A s^3 + (J_T R_A + bL_A)s^2 + (bL_A + K_T K_B)s} \quad (23)$$

C. Modelling of PID Controller

The objective of a control system is to achieve a fast response to a step input command with minimal overshoot and error. Solar tracking system motion control in this work is set forth as an electric motor motion control in terms of output angular displacement. This motion control system is to be developed analytically with feedback using a photo sensor, such that it ensures that the desired output position is met.

A typical structure of a PID control system is shown in Figure 3, where it can be seen that in a PID controller, the error signal *e(t)* is used to generate the proportional, integral, and derivative actions, with the resulting signals weighted and summed to form the control signal *u(t)* applied to the plant model.

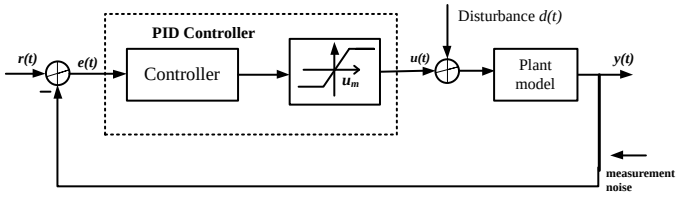

Figure 3: A typical PID control structure

A mathematical description of the PID controller is

International Journal of Engineering Research & Technology (IJERT)
ISSN: 2278-0181
Vol. 14 Issue 09, September - 2025

$$u(t) = K_P\left[e(t) + \frac{1}{T_i}\int_0^t e(\tau)d\tau + T_d\frac{de(t)}{dt}\right] \quad (24)$$

Where $u(t)$ is the input signal to the plant model, the error signal $e(t)$ is defined as $e(t) = r(t) - y(t)$, and $r(t)$ is the reference input signal.

In practical applications, the pure derivative action is never used, due to the "derivative kick" produced in the control signal for a step input, and to the undesirable noise amplification. It is usually replaced by a first-order low pass filter. Pre-filter is defined as a transfer function that filters the input signal prior to calculating the error signal. Thus, the Laplace transformation representation of the approximate PID controller can be written as in Equation 25

$$U(s) = K_P\left(1 + \frac{1}{T_i s} + \frac{sT_d}{1+s\frac{T_d}{N}}\right) \quad (25)$$

where N is the order of the low-pass pre-filter.

Adding the PID controller system to plant, will result in the addition of poles and/or zeros that will affect the response, mainly the added zero, will significantly and inversely affect the response and should be cancelled by pre-filter.

D. Modelling of Fuzzy Logic Controller

Fuzzy logic is an approach that closely mirrors human reasoning and decision-making processes. In contrast to conventional control strategies, which typically operate on precise point-to-point mappings, fuzzy logic controllers function on the principle of range-to-point or range-to-range mappings. The mechanism relies on the fuzzification of both inputs and outputs through associated membership functions. A crisp input is assigned varying degrees of membership across these functions, and the final output is determined by the aggregation of these memberships rather than a single deterministic value. Consequently, the controller's decision is influenced by a continuum of possible input states. This characteristic of fuzzy logic reflects its applicability to real-world situations, where ambiguity and imprecision are inherent. For instance, in survey responses, individuals often provide answers such as "Not Very Satisfied" or "Quite Satisfied," which cannot be quantitatively defined with absolute precision. Such linguistic variables represent vagueness that humans naturally employ in judgment, but which conventional machine-based control systems are unable to replicate effectively. The block diagram is shown in Figure 4.

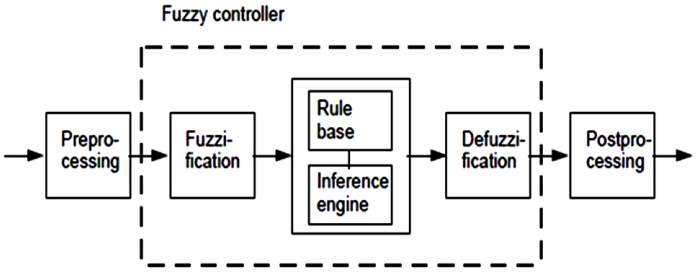

Figure 4: Fuzzy logic controller system

To implement the fuzzy logic technique in a real application requires the following three steps:

a. Fuzzification: convert classical data or crisp data into fuzzy data or Membership Functions (MFs).
b. Fuzzy Inference Process: combine membership functions with the control rules to derive the fuzzy output.
c. Defuzzification: Use different methods to calculate each associated output and put them into a table: the lookup table. Pick up the output from the lookup table based on the current input during an application.

IV. MODELS EXPERIMENTATION AND SIMULATION

In order to experiment with and analyse the mathematical models created in the preceding sections, this article used a virtual modelling environment called MATLAB and Simulink. The framework of the entire system is made up of the solar panel, solar angles, solar tracker, PID controller, and FLC controller, it is important to note. Conducting a comparison analysis to ascertain the efficacy of the designed controllers is the main goal of the simulation.

International Journal of Engineering Research & Technology (IJERT)
ISSN: 2278-0181
Vol. 14 Issue 09, September - 2025

A. Solar Tracker System Simulation

The continuous-time transfer function model of the solar tracking system, created in Equation 23, was ultimately represented in Simulink. For both horizontal and vertical panel direction control, the system consists of two DC permanent magnet motors.

$$\frac{\vartheta(s)}{V_{IN}(s)} = \frac{K_T K_A}{J_T L_A s^3 + (J_T R_A + b L_A) s^2 + (b L_A + K_T K_B) s}$$

In order to replicate the altitude and azimuth angles based on the calculated angles of the sun's incidence on the solar panel, a controller uses sets of two spur gears to lower the motor's speed.

Equation 23 was used to implement this continuous-time transfer function model, and Equation 26 represents the outcome of inserting these parameters.

KT = 0.1112; Torque constant (Nm/A))
KA = 1.38; Amplifier gain (V/m)
JT = 87.6855; Total moment of inertia (kg*m^2)
LA = 0.13; Armature inductance (H)
RA = 0.5; Armature resistance (Ohms)
b = 0.001; Viscous friction coefficient (Nm/KRPM)
KB = 0.1098; Back EMF constant

$$\frac{\vartheta(s)}{V_{IN}(s)} = \frac{0.1535}{11.39\, s^3 + 43.8 s^2 + 0.01234\, s} \tag{26}$$

The two PMDC motors that supply the necessary slew rate through the gear mechanism are powered by a 48V voltage, which is the tracker mechanism's input. The angular position is the output. To evaluate its response and ascertain how the PID controller tuning parameters and Fuzzy Logic controller universe of discourse worked, the tracker was simulated independently for a whole day.

B. Solar System Simulation with FLC

This paper used MATLAB and Simulink semantics to design the fuzzy logic controller. The initial step in FLC modelling is always to identify the discourse universe for the suggested controller. The altitude angles FL controller has two inputs: the altitude angles error and the rate at which this error changes. The output is the desired angle of incidence needed to maximise the amount of radiation that reaches the panels. The azimuthal angular errors, the rate at which these errors changed, and the actual horizontal angular movement of the panels were the inputs and outputs of the azimuthal angles FLC, respectively. A fixed solar panel array simulation was used to calculate the inputs and outputs for the azimuthal angular (FLC2) and altitude or elevation angular (FLC1) controllers. The FLC1 error universe of discourse is between -180^0 and 180^0, while the error change rate is between -19o and 19o. Furthermore, FLC2 error is between -550^0 and 550^0, and error change rate is between -36^0 and 36^0.

The rules-based table elevation FLC obtained is shown in Table 1. This is the same as the azimuthal FLC

Table 1: Fuzzy-based initial rules for elevation FLC

	Elevation Angular Error (E)							
Elevation Error Change (ΔE)		NL	NM	NS	Z	PS	PM	PL
	NL	NL	NL	NL	NL	NM	NS	Z
	NM	NL	NL	NL	NM	NS	Z	PS
	NS	NL	NL	NM	NS	Z	PS	PM
	Z	NL	NM	NS	Z	PS	PM	PL
	PS	NM	NS	Z	PS	PM	PL	PL
	PM	NS	Z	PS	PM	PL	PL	PL
	PL	Z	PS	PM	PL	PL	PL	PL

International Journal of Engineering Research & Technology (IJERT)
ISSN: 2278-0181
Vol. 14 Issue 09, September - 2025

The rules were developed using a fuzzy logic toolbox and subsequently translated into the table presented above. In Table 2, the grey-colored row and column denote the linguistic terms that form the antecedents of fuzzy rules concerning the heuristic variables: elevation error, azimuthal error, change in elevation error, and azimuthal error. The central portion of the table, featuring a transparent background, represents the consequences of the rules. The 49 established rules are implemented in MATLAB. However, the numerous rule bases have led to increased computational time, slower implementation of the controller, and reduced efficiency. To enhance the execution speed of the controller and decrease its response time, the 49 rules were condensed to 16 rule bases for the two controllers.

V. RESULT AND DISCUSSION

The final analogy in this paper was to briefly compare the results of these different tracking systems with the sole aim of finding which of them has a better performance, given all the developed models. It is important to display the values of the solar panel generated current and voltages as illustrated in Tables 2 and 3.

Table 2: Currents generated for different tracking systems

Currents (A)			
Time (Hours)	Fixed-Axis Tracking	Two-Axis with PID	Two-Axis with FLC
6	1.0000	8.6663	12.9995
7	2.4529	8.7755	13.1628
8	5.7756	9.2200	13.8279
9	6.7542	10.1129	15.1635
10	7.1748	11.6408	17.4154
11	7.3664	13.7639	20.5376
12	7.3911	15.0516	22.3233
13	7.3411	13.7639	20.4670
14	7.1257	11.6408	17.2958
15	6.6849	10.1129	15.0075
16	5.7066	9.2200	13.6620
17	2.4319	8.7604	13.0500
18	1.5000	8.6364	12.8207

Table 3: Voltages generated for different tracking systems

Voltages (V)			
Time (Hours)	Fixed-Axis Tracking	Two-Axis with PID	Two-Axis with FLC
6	0	0	0
7	1.9043	6.8129	10.2190
8	8.9525	14.2914	21.4339
9	15.6769	23.4728	35.1955
10	22.2045	35.9636	53.8968
11	28.4971	53.0579	79.4432
12	34.4296	69.2862	103.6852
13	39.7595	73.4036	109.9300
14	44.1056	71.0470	106.4819
15	46.5493	69.4137	104.0824
16	44.1534	45.3215	83.7931
17	20.5922	20.4562	57.1917
18	4.5000	7.0123	15.4821

International Journal of Engineering Research & Technology (IJERT)
ISSN: 2278-0181
Vol. 14 Issue 09, September - 2025

All the performance curves for these systems are shown in Figures 5 and 6, respectively.

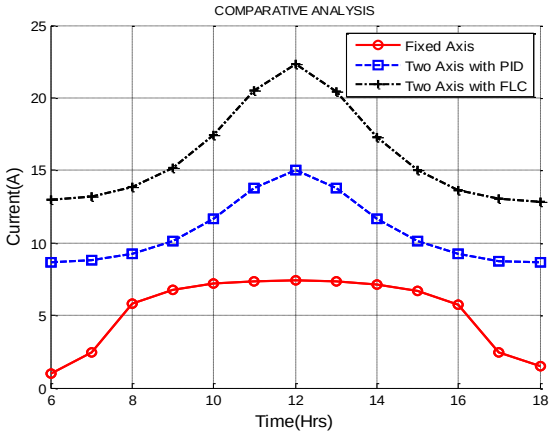

Figure 5: Comparison of solar panel-generated current.

Figure 5 shows the current (A) that the photovoltaic system makes during the day (6:00 to 18:00) in three distinct ways: Fixed-Axis Tracking, Two-Axis with PID controller, and Two-Axis with Fuzzy Logic Controller (FLC). The fixed-axis system made the least amount of current during the day, from 1.00 A in the early morning to a high of about 7.39 A at midday (12:00). The output went up steadily from 6:00 AM to noon. Then, it went down a little bit till evening, when it dropped back to 1.50 A around 18:00. This pattern shows how the fixed-axis panel's poor alignment with the sun's position makes it less able to capture energy.

The PID-based system made a lot more current than the fixed-axis system. The current went up from 8.67 A at 6:00 to a peak of 15.05 A at noon (12:00) before slowly falling to 8.64 A at 18:00. The curve shows how well PID control works to make it easier to collect energy and follow the sun more closely. When the system was at its busiest, the PID system usually gave out almost twice as much current as the fixed-axis system.

The FLC-based tracker always did better than both the PID and fixed-axis systems, no matter what time of day it was. At 06:00, the current production started at 13.00 A. It peaked at 22.32 A at 12:00 and then dropped to 12.82 A at 18:00. The FLC tracker reached the maximum peak current and kept up its great performance throughout the morning and evening. This shows how strong and adaptable it is to changing irradiance conditions. The average current over the course of the day was far higher than that of either PID or fixed-axis, showing that it was better.

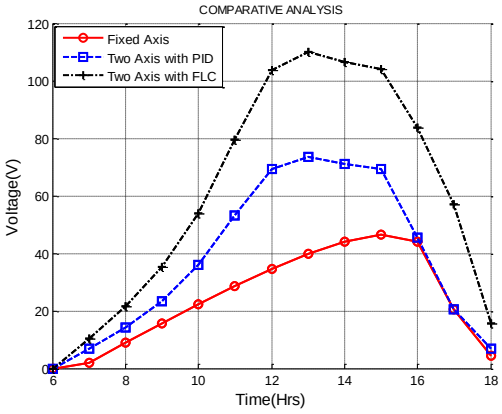

Figure 6: Comparison of solar panel-generated voltages

Figure 6 shows the voltage outputs of three solar tracking setups: a fixed-axis tracker, a two-axis tracker with Proportional–Integral–Derivative (PID) control, and a two-axis tracker with Fuzzy Logic Control (FLC). From 6:00 to 18:00, the data was collected. The results show that the systems work in distinct ways. The tracker that uses FLC works best all day.

All systems showed zero volts at 6:00 h because there wasn't much sunshine at dawn. The systems started generating voltages that could be measured at 7:00 h. The fixed-axis system only made 1.90 V, but the PID and FLC systems made more: 6.81 V and 10.22 V, respectively. This early difference in performance shows that active tracking systems are better at picking up low-angle morning radiation than fixed systems.

International Journal of Engineering Research & Technology (IJERT)
ISSN: 2278-0181
Vol. 14 Issue 09, September - 2025

From 8:00 to 12:00, all systems showed a quick spike in voltage output. This was in keeping with the steady rise in solar radiation. The fixed-axis tracker reported 34.43 V at 12:00 h, and the PID-controlled two-axis tracker read 69.29 V. The FLC-based tracker had the greatest output of 103.69 V, which is more than three times that of the fixed-axis system and nearly 1.5 times that of the PID system. This result shows that the FLC controller does a better job of keeping the panels in the right spot when the sun is at its highest point.

Between 12:00 and 14:00, the voltages from all three systems were at their maximum. The fixed-axis tracker hit its highest point around 15:00 h, when it was at 46.55 V. The PID system achieved its greatest point around 13:00 h, when it was 73.40 V. At 1:00 PM, the voltage in the FLC system reached its highest point, 109.93 V. It stayed more stable than the PID system, which started to drop off faster at 14:00. The FLC's performance during peak hours shows that it can handle changes in irradiance well, which is important for maintaining power generation steady.

The voltage outputs of all systems were lower after 15:00 h since the sun was getting less brilliant. The FLC system, on the other hand, had voltages that were higher than those of the PID and fixed-axis systems. For example, at 17:00 h, the fixed-axis and PID trackers put out 20.59 V and 20.46 V, while the FLC system kept functioning and put out 57.19 V, which was a lot more. The FLC tracker made 15.48 V around 18:00, which was near to sunset. The PID system only made 7.01 V, and the fixed-axis tracker only made 4.50 V.

The results show that the FLC-based two-axis tracker always works better than the PID-based tracker and the fixed-axis system, no matter what time of day it is. The FLC tracker not only had the highest maximum voltage output (109.93 V), but it also worked better throughout both low-irradiance hours (morning and evening) and peak-irradiance hours. These results show that fuzzy logic control is a better way to keep track of solar energy since it is more adaptable, more precise when making changes to angles, and less impacted by changes in solar circumstances.

VI. CONCLUSION

This study employs MATLAB/Simulink simulations to evaluate the efficacy of fixed-axis, two-axis PID-controlled, and two-axis fuzzy logic-controlled (FLC) solar tracking systems in Nigeria. We have constructed mathematical models for the solar array, the angles at which the sun tracks, the tracker drive mechanism, the PID controller, and the fuzzy logic controller (FLC). The simulations go for an entire day, and the voltages and currents they make are looked at. The findings show that the FLC-based tracker always works better than the PID-controlled and fixed-axis systems during the day. The FLC tracker has the highest peak current (22.32 A) and voltage (109.93 V) and performs better than any other tracker when the sun is shining brightly or not at all. The PID-controlled system also indicates that it can get more energy than the system with a fixed axis. The research indicates that fuzzy logic control is a superior method for measuring solar energy in Nigeria, where sunlight levels fluctuate continuously.

VII. REFERENCES

[1]. Issa, H. A. (2025). Design, modeling and control of a dual-axis solar tracker. Journal of Engineering Research/ ScienceDirect.
[2] Kumba, K. (2024). Solar tracking systems: Advancements, challenges, and adoption pathways. Energy Reports / Review.
[3] Sadeghi, R., Parenti, M., & Fossa, M. (2025). A review and comparative analysis of solar tracking systems. Energies, 18(10), 2553.
[4] Eyibo, N. R., Nkan, I. E., Jack, A. L., & Johnson, E. H. (2025). Design, simulation and analysis of a 3 MW grid-connected solar PV system in Nigeria using MATLAB/Simulink. Journal of Engineering Research and Reports, 27(4), 291–304.
[5] Arora, P., Singh, R., & Verma, S. (2021). Comparative performance of fuzzy and PID controllers in solar tracking. Solar Energy, 221, 350–359. https://doi.org/10.1016/j.solener.2021.05.014
[6] Hassan, M., Ali, R., & Zhou, Y. (2022). Hybrid PID–fuzzy control for dual-axis solar trackers under variable weather conditions. Renewable Energy, 185, 1204–1216.
[7] Sharma, A., & Kumar, N. (2023). Intelligent controller design for PV tracking: A comparative study. Energy Reports, 9, 215–225.
[8] Li, Q., Zhao, J., & Wu, F. (2021). ANFIS-based solar tracking system for enhanced energy yield. Applied Energy, 301, 117453.
[9] Mahdavi, S., & Rezaei, M. (2024). Intelligent solar tracking with ANFIS: Performance and cost analysis. Journal of Cleaner Production, 412, 137025.
[10] Zhang, L., Chen, D., & Yang, H. (2021). Modeling and simulation of fuzzy-controlled solar trackers in MATLAB/Simulink. Energy Conversion and Management, 245, 114611.
[11] Mwangi, J., Otieno, D., & Kamau, P. (2022). Simulation and performance analysis of solar trackers in sub-Saharan Africa. Renewable and Sustainable Energy Reviews, 157, 112038.
[12] Wang, Y., & He, X. (2023). Particle swarm optimization of PID controllers for solar tracking. Control Engineering Practice, 135, 105454.
[13] Adeyemi, T., Okeke, C., & Balogun, O. (2024). GA-optimized fuzzy logic controllers for solar tracking in Nigeria. International Journal of Electrical Power & Energy Systems, 153, 109015
[14] Okafor, J., & Eze, C. (2023). Reliability modeling of solar trackers under fault conditions. IEEE Access, 11, 54120–54133.
[`15] Khan, S., Ahmed, I., & Ali, H. (2022). Low-cost fuzzy logic solar tracker for rural electrification. Energy for Sustainable Development, 69, 180–188.
[16] Aliyu, M., & Ibrahim, U. (2023). Design and performance evaluation of a PID-based dual-axis solar tracker in Nigeria. Nigerian Journal of Engineering, 30(2), 45–55.
[17] Singh, R., & Patel, V. (2024). Field validation of hybrid PID–fuzzy solar tracking systems in India. Solar Energy Materials & Solar Cells, 259, 112374.
[18] Lopes, L. A. C and Lienhardt, A. M. (2003). A Simplify Nonlinear Power Source for Simulating PV panels. In: 34th Annual World Conference of IEEE on Power Electronics Specialist, 1729-1734.